FIRST COLD TESTS OF THE SUPERCONDUCTING CW DEMONSTRATOR AT GSI

F. Dziuba[1,*], M. Amberg[1,3,†], K. Aulenbacher[1,4], W. Barth[1,2,5], M. Basten[3], M. Busch[3], V. Gettmann[1], M. Heilmann[2], S. Mickat[2], M. Miski-Oglu[1], H. Podlech[3], M. Schwarz[3], S. Yaramyshev[2,5]

[1]HIM Helmholtz Institute Mainz, 55099 Mainz, Germany
[2]GSI Helmholtzzentrum für Schwerionenforschung GmbH, 64291 Darmstadt, Germany
[3]IAP Goethe University Frankfurt, 60438 Frankfurt am Main, Germany
[4]KPH Johannes Gutenberg University Mainz, 55128 Mainz, Germany
[5]MEPhI National Research Nuclear University, 115409 Moscow, Russia

Abstract

The future experimental program of super heavy element synthesis at GSI desires high intense heavy ion beams at or above the coulomb barrier, exceeding the capabilities of the GSI-UNILAC (Universal Linear Accelerator). Additionally, the existing GSI accelerator chain will be used as an injector for FAIR (Facility for Antiproton and Ion Research) primarily providing high power heavy ion beams at a low repetition rate. Due to this limitations a new dedicated superconducting (sc) continuous wave (cw) linac is proposed to keep the Super Heavy Element (SHE) research program at GSI competitive. The construction of the first linac section has been finished in the 3rd quarter of 2016. It serves as a prototype to demonstrate its reliable operability in a realistic accelerator environment. This demonstrator cryomodule comprises the sc 217 MHz crossbar-H-mode (CH) multigap cavity as the key component of the whole project and two sc 9.3 T solenoids. The performance of the cavity has been extensively tested at cryogenic temperatures. In this contribution the measurement results of initial cold tests will be presented.

INTRODUCTION

Regarding the future construction of a sc cw linac at GSI an R&D program has been initiated. It is intended to build and test the first linac section with beam [1]. In this context, a sc 217 MHz CH cavity [2] with 15 equidistant accelerating cells, $\beta = 0.059$ was built (see Table 1). The beam dynamics layout of the cavity is based on the special EQUUS (EQUidistant mUlti-gap Structure) [3]. Three dynamic bellow tuners inside the cavity adjust frequency changes during operation [4]. Furthermore, a helium vessel made from titanium provides a closed helium circulation around the cavity. Several flanges in each quadrant of the cavity allow an adequate surface processing. For future beam tests a 5 kW cw power coupler is available. After final surface preparation steps the new cavity has been extensively tested with low level rf power at 4.2 K.

Table 1: Main parameters of the cavity

β (v/c)		0.059
Frequency	MHz	216.816
Accelerating cells		15
Effective length ($\beta\lambda$)	mm	612
Diameter	mm	409
Tube aperture	mm	18 / 20
G	Ω	52
R_a/Q_0		3240
$R_a R_S$	kΩ^2	168
E_a (design)	MV/m	5.5
E_p/E_a		6.3
B_p/E_a	mT/(MV/m)	5.7

RF TESTS OF THE CAVITY

A first rf test of the sc 217 MHz CH cavity (without helium vessel) at the Institute of Applied Physics (IAP) of Goethe University Frankfurt has been performed beginning of 2016 [5]. At that time the performance of the cavity was limited by field emission caused by insufficient surface preparation. Regarding this, rinsing could be performed along the beam axis only. Due to a technical re-

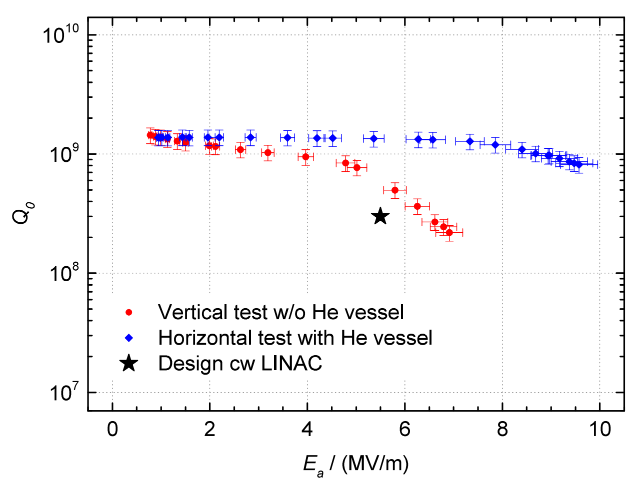

Figure 1: Q_0 vs. E_a curves at 4.2 K for two different rf tests.

* f.dziuba@gsi.de
† out of business

ISBN 978-3-95450-181-6

Copyright © 2017 CC-BY-3.0 and by the respective authors

striction of the provided High Pressure Rinsing (HPR) device, rinsing was not possible inside each quadrant of the cavity. Nevertheless, a maximum accelerating gradient of $E_a = 6.9$ MV/m at $Q_0 = 2.19 \cdot 10^8$ was reached (see Figure 1).

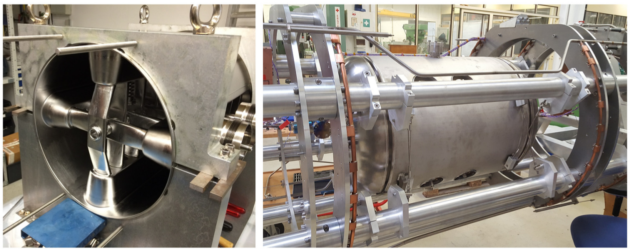

Figure 2: Superconducting 217 MHz CH Cavity during manufacturing (left) and finally mounted into the support frame (right).

After the final assembly of the helium vessel and further HPR preparation the cavity was delivered to GSI and prepared for a second rf test in a horizontal cryomodule (see Figure 2). A 50 W broadband amplifier was used to deliver the required rf power. The cavity was operated as a generator driven resonator directed by an rf control system. Further equipment, namely a network analyzer, three power meters and a scope has been used for rf measurements. To validate the measuring system all power meters have been calibrated via the X-ray spectrum of the cavity recorded at a gradient of 5.5 MV/m. X-rays arise from field emission; it is assumed that electrons, coming from the drift tube where the highest voltage is located, are accelerated to the neighbouring tube inside the cavity. Consequently, a continuous Bremsstrahlung spectrum is generated by hitting the neighbouring drift tube. The maximum energy as well as the maximum electron energy of the measured sprectrum was 574 keV (see Figure 3), confirmed by the related absolute voltage determined by the power meters (567 ± 7 kV).

Initially, the cavity has been passively precooled down to 218 K by the N_2 shield of the cryostat. Hereafter, the temperature was quickly lowered (3 K/min in average) applied by liquid helium to 4.2 K avoiding hydrogen related Q-disease. A mean residual pressure of $4 \cdot 10^{-9}$ mbar could be achieved applying evacuation by a turbomolecular and an ion getter pump. Subsequently, rf conditioning has been performed. All multipacting barriers up to 4 MV/m could permanently be surmounted.

In a next step the rf performance of the cavity was reviewed. Figure 1 shows the related Q_0 vs. E_a curves measured in vertical position (without helium vessel, red curve) and in horizontal orientation (with helium vessel, blue curve), respectively. The maximum Q-value at a low field level (Q_0^{low}) was measured for $1.37 \cdot 10^9$ which is 4.9 % lower in comparison to the first vertical test. This minor discrepancy is caused by worse magnetic shielding leading to a less residual surface resistance R_S (38 nΩ instead of 36 nΩ, see Table 2). Nevertheless, recently the cavity showed an improved performance due to an advanced HPR treatment. The initial design quality factor at 5.5 MV/m has been exceeded by a factor of 4. Furthermore, a maximum accelerating gradient of $E_a = 9.6$ MV/m at $Q_0 = 8.14 \cdot 10^8$ was reached, which is a promising result considering the complex multigap structure of the cavity. The maximum gradient is limited by cavity quenches presumably caused by a thermal defect since the degeneration of the Q-value is still quite low. Table 2 summarizes the main measurement results of both rf tests.

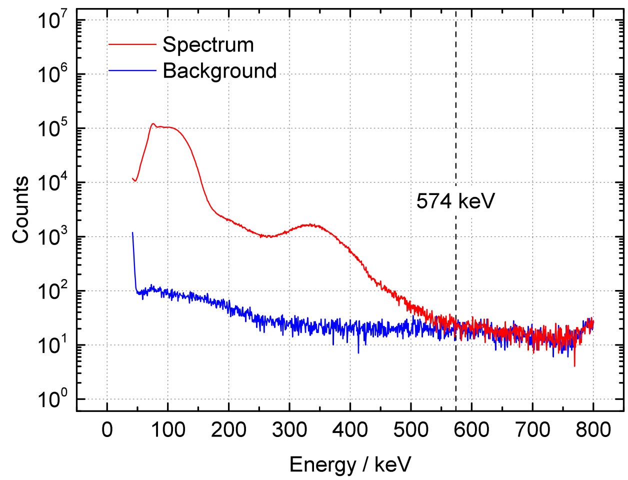

Figure 3: X-ray spectrum of the cavity at $E_a = 5.5$ MV/m.

Table 2: Main results of the vertical and horizontal rf test

		Vertical test w/o He vessel	Horizontal test with He vessel
Q_0^{low}		$1.44 \cdot 10^9$	$1.37 \cdot 10^9$
R_S	nΩ	36	38
R_{BCS}	nΩ	15	15
R_{mag}	nΩ	9	12
R_0	nΩ	12	11
E_a	MV/m	6.9	9.6
Q_0		$2.19 \cdot 10^8$	$8.14 \cdot 10^8$
V_a	MV	4.2	5.9
E_p	MV/m	43	60
B_p	mT	39	55

FURTHER ANALYSIS

Respectively the evaluation of the power consumption shows that the cavity was no longer limited by field emission at low field levels contrary to earlier measurements. Figure 4 shows the total power losses inside the cavity as function of the gradient in comparison to the expected ohmic losses asuming a constant Q-value. Related to the previous test (red curve) the total losses increase due to field emission from $E_a = 2$ MV/m while the related peak electric field E_p is estimated in the range between 12 MV/m or 43 MV/m referred to the maximum gradient. At $E_a = 5$ MV/m

Copyright © 2017 CC-BY-3.0 and by the respective authors

ISBN 978-3-95450-181-6

repectively at $E_p = 32$ MV/m the total power consumption increases rapidly suggesting an activation of a field emitter. This behaviour can be confirmed by considering the corresponding non-ohmic losses which increase exponentially starting at the same field level as shown in Figure 5. After the cavity's surface was rinsed again a central field emitter could be removed or at least significantly smoothed. Thus, extremely reduced non-ohmic losses occur and a minor field emitter activation only beyond $E_a = 7.8$ MV/m can be observed (see Figure 5, blue curve). In that case E_p is 49 MV/m or up to 60 MV/m at the maximum accelerating gradient. Figure 6 shows the corresponding Fowler-Nordheim plot illustrating the different enhancement factors β_{FN} of the emitting spots for the two different surface qualities. Due to the extensive HPR treatment and the resulting improvment of the surface quality the enhancement factor could be decreased from $\beta_{FN} = 403$ to $\beta_{FN} = 176$ reflecting a distinct difference in emitter activity.

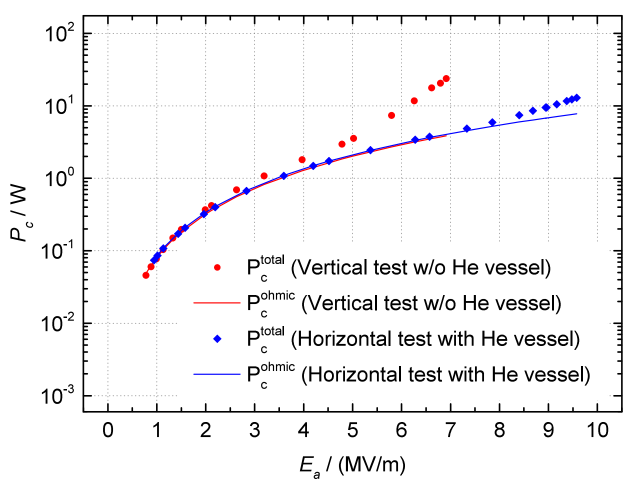

Figure 4: Total losses inside the cavity in comparison to pure ohmic losses for the vertical and horizontal rf test.

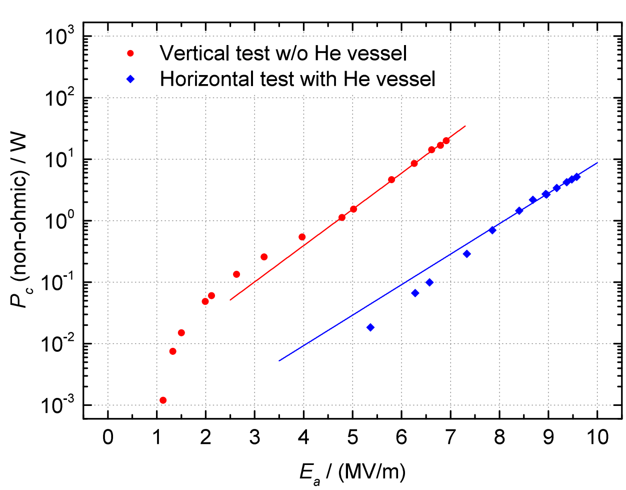

Figure 5: Non-ohmic losses inside the cavity before and after the improved surface preparation.

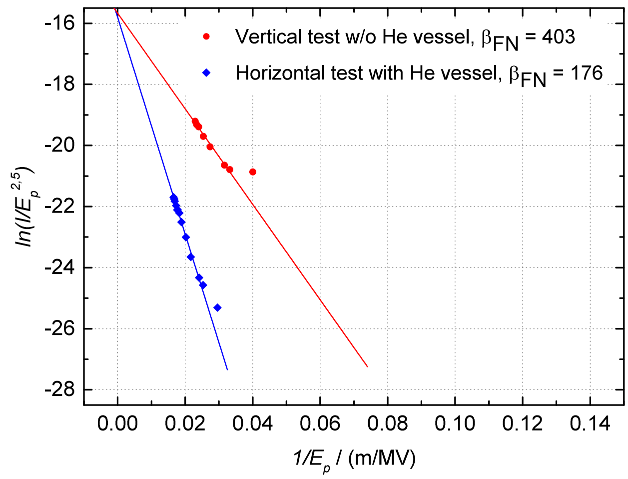

Figure 6: Fowler-Nordheim plot for the two different surface qualities.

SUMMARY & OUTLOOK

The sc 217 MHz CH cavity has been successfully tested at GSI with low level rf power at 4.2 K. A very promising gradient of 9.6 MV/m could be reached after an advanced surface preparation. In a next step a full performance test with beam is planned for the 1st quarter of 2017. Afterwards an optimized HPR device will be used allowing to rinse the cavity additionally inside each quadrant. Other methods, like an argon plasma discharge or a 300°C bake-out, are foreseen to improve the surface quality of the cavity. Furthermore, two short sc 217 MHz CH cavities [6] with a simplified geometry for the advanced demonstrator [7,8] are currently under construction, at least reproducing or probably improving the excellent results made so far.

REFERENCES

[1] V. Gettmann et al., in Proc. of SRF2011, Chicago, Illinois, USA, MOPO030 (2011).

[2] F. Dziuba et al., Phys. Rev. ST Accel. Beams 13, 041302 (2010).

[3] S. Minaev et al., Phys. Rev. ST Accel. Beams 12, 120101 (2009).

[4] M. Amberg et al., in Proc. of LINAC2014, Geneva, Switzerland, MOPP068 (2014).

[5] F. Dziuba et al., in Proc. of LINAC2016, East Lansing, Michigan, USA, THPLR044 (2016).

[6] M. Basten et al., in Proc. of IPAC2016, Busan, Korea, MOPOY019 (2016).

[7] W. Barth et al., in Proc. of IPAC2014, Dresden, Germany, THPME004 (2014).

[8] W. Barth et al., in Proc. of Baldin ISHEPP XXIII, Dubna, Russia, EPJ Web of Conferences (in press) (2016).

Copyright © 2017 CC-BY-3.0 and by the respective authors

ISBN 978-3-95450-181-6